ChemComm

COMMUNICATION

View Article Online
View Journal | View Issue

Cite this: *Chem. Commun.*, 2022, 58, 13731

Received 25th October 2022,
Accepted 14th November 2022

DOI: 10.1039/d2cc05788c

rsc.li/chemcomm

A dynamic reversible phenylboronic acid sensor for real-time determination of protein–carbohydrate interactions on living cancer cells†

Quanquan Song,‡[a] Qian Li,‡[a] Shuang Chao,[a] Xian Chen,[a] Ronghui Li,[b] Yuchao Lu,*[b] Teodor Aastrup[c] and Zhichao Pei*[a]

Real-time detection of glycosylation on label-free cancer cell surfaces is of significance for the diagnosis and treatment of cancer. In this work, we have successfully developed a novel dynamic reversible sensor based on pH-sensitive phenylboronic esters to determine in real-time the binding kinetics of protein–carbohydrate interactions on suspension cancer cell surfaces using a quartz crystal microbalance (QCM) technique.

Cell surface glycosylation is involved in many important physiological processes of organisms, including cell proliferation, differentiation, migration, cell–cell recognition, immunomodulation and signal transduction.[1–4] The abnormal expression of glycosylation is closely associated with many pathological conditions including cancer, as it regulates the development and progression of cancer and also serves as an important biomarker for cancer diagnosis and treatment.[5–9] Therefore, it is of great significance to determine cancer cell surface glycosylation for the investigation of carcinogenic mechanisms and therapeutic approaches.[10,11] Currently, there are already some methods and techniques to study cell surface glycosylation like electrochemistry,[12] fluorescence spectroscopy[13,14] as well as biosensor technologies, such as microarray,[15] microfluidic control,[16,17] surface plasma resonance (SPR)[18,19] and quartz crystal microbalance (QCM) techniques.[20,21] However, conventional methods usually require the separation and purification of glycosylated molecules on cell surfaces, which is not only complicated and time-consuming, but also has a risk of destroying the glycosylated molecule structures, leading to a lack of authenticity and accuracy in the data.

In order to directly detect cell surface glycosylation, various strategies involving many dynamic reversible chemical bonds (hydrogen bonds, electrostatic effects, reversible boronic esters, benzoicimine bonds and photosensitive nitrophenyls, *etc.*) to construct chemosensors have been exploited.[22–26] QCM cell-based biosensors have the characteristics of showing high sensitivity, without the need to purify them and they are also label-free.[27] Cells can be immobilized on the sensor surface directly, which provides more authentic and accurate data for cell surface glycosylation studies.[28] In our previous studies, suspension cancer cells were captured onto the sensor surface by the interaction of Concanavalin A (Con A) and cell surface carbohydrates.[29] Insufficiently, the exposed Con A on the sensor surface (without being completely covered by cells) would interfere with the detection of biomolecules with glucose/mannose structures. Furthermore, suspension cells were immobilized directly onto a polydopamine-coated sensor by Michael addition and Schiff base reactions.[30] Compared to the above method, this method does not interfere with the detection of biomolecules, but it leads to cell-death through covalent bonding. Therefore, it is highly desirable to develop a QCM living cell biosensor with non-interference for real-time detection of cell surface glycosylation.

Boronic acid can realize the site-specific bioconjugation of glycoproteins through reversible covalent bonding with glycosylation sites, which depend on the fast and stable formation of boronic esters (five- or six- membered cyclic complexes) between boronic acid and 1,2-/1,3-*cis*-diol structures in cell surface bioligands. Among of them, phenylboronic esters have been frequently used to fabricate sensor chips for glycoprotein analysis,[31] glucose detection,[32] and controllable cell adhesion.[33,34] Hence, we designed a dynamic reversible phenylboronic acid sensor, which can capture living suspension cells through the phenylboronic ester biomaterial interfaces formed by dynamic reversible covalent complexation between

[a] *Shaanxi Key Laboratory of Natural Products & Chemical Biology, College of Chemistry & Pharmacy, Northwest A&F University, Yangling 712100, P. R. China. E-mail: peizc@nwafu.edu.cn*
[b] *Hebei Key Laboratory of Analysis and Control of Zoonotic Pathogenic Microorganism and College of Science & Technology, Hebei Agricultural University, Huanghua, Hebei 061100, China. E-mail: luyuchao@hebau.edu.cn*
[c] *Attana, Stockholm SE-11419, Sweden*

† Electronic supplementary information (ESI) available. See DOI: https://doi.org/10.1039/d2cc05788c

‡ These authors contributed equally.

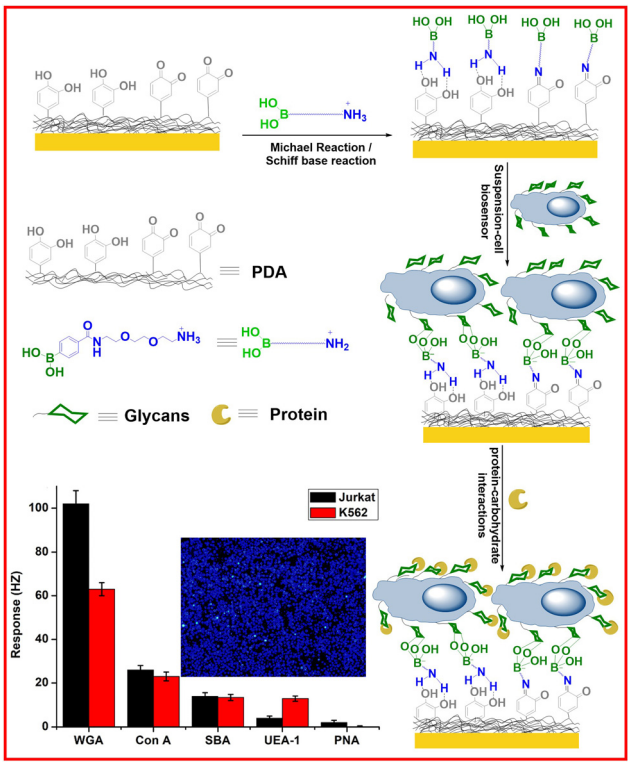

Scheme 1 Schematic illustration of the PBA-based suspension-cell QCM biosensor for real-time detection of lectin–cells interactions.

cis-diol-containing structures on cell surfaces by glycosylation. In addition, the sensor could be regenerated by fructose competition due to the fact that fructose has a particularly high affinity for aryl boronic acids in the range of pH 7–9. The bound fructose was then removed by treatment with phosphate at low pH due to the pH-sensitive boronic esters. This has greatly improved the potential applications of the sensor and has reduced the cost of use.[35] Two kinds of suspension cancer cells, human acute lymphocytic leukemia Jurkat cells (Jurkat cells) and human acute myeloid leukemia K562 cells (K562 cells) were measured with several lectins to evaluate the cell surface glycosylation, and the binding kinetics of the lectin–glycan interactions were analyzed in real-time by the cell-based QCM biosensor (Scheme 1).

Firstly, polydopamine was coated on the gold sensor chip after dopamine incubation. The thickness of the polydopamine film on the gold chip surface was 65.91 nm, measured by a PZ 2000 ellipsometer. Simultaneously, the surface morphology of the sensor surface was characterized by AFM before and after the polydopamine coating (Fig. S5 and S6, ESI†). After the polydopamine coating, the R_q of the sensor surface changed from 4.59 nm to 6.90 nm and aggregated polydopamine nanoparticles could be observed. Next, compound **3** (phenylboronic acid derivative, PBA) was synthesized from 2,2′-(ethylene dioxy)-bis(ethylamine) and 4-carboxyphenyl boric acid (for details of the synthesis see Fig. 1). Then, the PBA was fixed on the polydopamine-coated chip by Michael addition and Schiff base reactions, to prepare the PBA functionalized sensor chip (PBA-chip). The PBA-chip morphology was determined by SEM–EDS

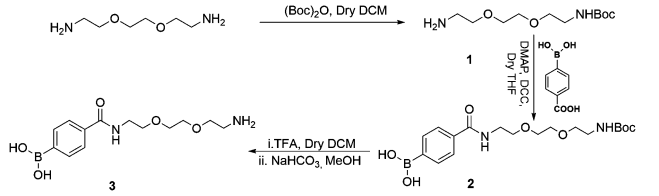

Fig. 1 The synthesis route of compound **3** (PBA).

and SEM (Fig. S7, ESI†). Compared with a gold sensor chip (Fig. S7(a) and (c), ESI†), the PBA-chip had more C, H, O, N and B elements (Fig. S7(b) and (d), ESI†), which indicated that polydopamine and PBA were successfully immobilized on the chip surface. Moreover, the PBA functionalized sensor chip was investigated by FT–IR spectroscopy (Fig. S8, ESI†), which showed an absorption band at 3157 cm^{-1} corresponding to the –OH stretching mode of the phenylboronic acid, confirming the presence of PBA units on the sensor chips.

Jurkat cells were captured by the PBA-chip and were observed with SEM (Fig. S9, ESI†), then stained with Hoechst 33258 and observed under a fluorescence microscope (Fig. 2a). The results showed that Jurkat cells were successfully captured on the sensor surface with good activity and uniform distribution. PBA is able to immobilize cells by forming boronic esters with *cis*-diol-containing structures on the cell surfaces.[36,37] This chemical bond is pH-sensitive, which is stable at pH 6.8–7.5 and breaks at pH < 5.5.[38,39] Following the QCM measurements, the QCM Jurkat cell sensor's regeneration was examined by competing with 20 mM fructose solutions at pH 8.5 and then incubating with PBS (1 mL) at pH 3.0 for 1 h at room temperature.[40] The cells were stained again and observed with fluorescence microscopy (Fig. 2b). As seen in the Fig. 2b, there

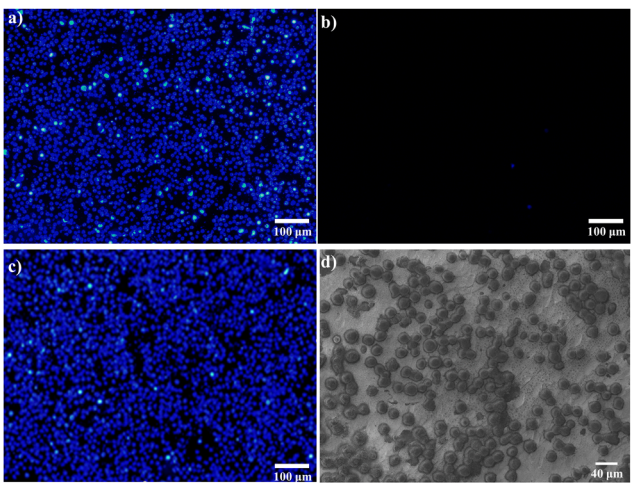

Fig. 2 Fluorescence images of (a) the PBA-based suspension-cell sensor surface, on which the Jurkat cells were captured by boronic acid groups and fixed on the chip, (b) the Jurkat cells that were eluted from the chip by 20 mM fructose; after the sensor chip was regenerated, (c) the Jurkat cells were captured again and successfully fixed. (d) The SEM image of the Jurkat cells that were captured again. As counted using ImageJ software, the cell coverage had no significant changes before and after QCM measurements (a: 2.16×10^5 cells per cm^2, c: 2.19×10^5 cells per cm^2).

were a few cells on the surface, indicating that the cells were successfully removed from the chip.[12] Furthermore, the sensors were regenerated (Fig. S10, ESI†), Jurkat cells were incubated again on the PBA-chip surface, stained and observed by fluorescence microscopy (Fig. 2c) and SEM (Fig. 2d). Notably, there was no significant change of the cell coverage on the sensor surface after regeneration (a: 2.16 × 10^5 cells per cm^2, c: 2.19 × 10^5 cells per cm^2, counted with ImageJ software), which indicated that the suspension cells that attached to the sensor surface had excellent stability, capability and ability to be regenerated for capturing cells. These results showed that Jurkat cells were successfully captured again on the chip surface with good activity and uniform distribution, indicating that regeneration of the PBA chip was achievable and effective.

As an important tool for studying glycosylation on cancer cell surfaces, lectins can recognize and bind the specific structure of glycan.[41–43] Cell surface glycosylation can be evaluated by detecting the interaction between a series of lectins and cells using QCM biosensor techniques. Jurkat and K562 suspension cancer cell biosensors were docked into the QCM instrument. Five lectins were introduced to the sensor surface respectively, including Con A, wheat germ agglutinin (WGA), peanut agglutinin (PNA), soybean agglutinin (SBA) and Ulex europaeus agglutinin I (UEA-I) that specifically recognizes and binds mannose, *N*-acetylglucosamine (GlcNAc), galactoside, *N*-acetyl-galactosamine (*N*-GalNAc) and L-fucose. Each lectin was injected and run for 400 s, then the corresponding glycose was injected to competitively bind to the lectin. The process was repeated 2–3 times. Fig. 3a showed the binding and dissociation process of the Jurkat cells with 50 μg mL^{-1} WGA which was performed twice and the data was similar each time. The results indicated that the Jurkat cell sensor chip was reproducible and the method was reliable. The interactions of each lectin with the surface glycans of the Jurkat and K562 cells were subsequently tested separately and the mean frequency shifts were recorded and summarized (Fig. 3b). As can be seen, the different frequency shifts produced from the interactions between the lectins and the cell surfaces resulted from different glycosylation on the cell surfaces. This measurement of the responses obtained for each of the lectins to the living cell

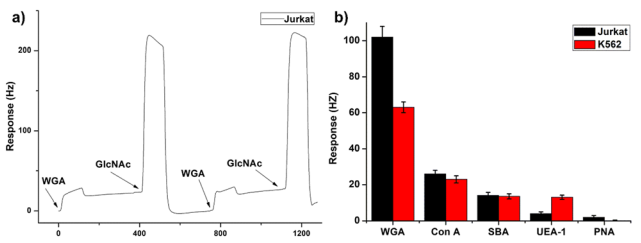

Fig. 3 (a) Frequency shift recorded during the binding and regeneration of WGA to Jurkat cell sensor surfaces. (b) Lectins (Con A, WGA, PNA, SBA and UEA-I) were injected over two different cell surfaces (Jurkat and K562 cells), respectively. The maximum frequency shift observed at the end of the injection phase was monitored. The data are representative of 3 independent experiments from 3 chips and are presented as the mean ± s.d.

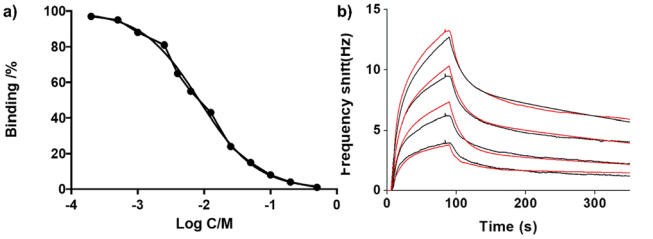

Fig. 4 (a) Competitive inhibition of the interaction of Con A with Jurkat cells using D-mannose as the competitor. (b) Kinetic evaluation of the interaction of SBA with Jurkat cells. SBA at 25, 50, 75 and 100 μg mL^{-1} (0.12, 0.24, 0.48 and 0.96 μM) were tested. The responses were recorded (black curves) and were globally fitted to a theoretical 1 : 2 binding model with a mass transport parameter (red curves).

surfaces enabled a real-time analysis of the lectin–cell interactions. In addition, it is well known that Con A can recognize and specifically bind to mannose. In this study, D-mannose was used as a competitive inhibitor to study the competitive inhibition of D-mannose on the binding of Con A to carbohydrates on the Jurkat cell surfaces. A mixture of 50 μg mL^{-1} Con A and a series of concentrations of D-mannose (0–495 mM) were injected onto the surface of the suspension-cell sensor. The binding of Con A gradually decreased with the increase of D-mannose due to the competitive effect of D-mannose (Fig. 4a). The result indicated that Con A was bound to mannose on the Jurkat cell surface, and the binding was specific. The half inhibitory concentration IC_{50} was 8.5 mM.

The kinetic study of the interactions between biomolecules and cells gave an insight into the cell surface glycosylation structures, which is important in the fields of disease diagnosis and drug development. The kinetics of the interactions between lectins and the cell surface glycans were measured by injecting WGA and SBA onto the sensor surface at 25, 50, 75 and 100 μg mL^{-1}, respectively. Fig. 4b showed the kinetic study of SBA and Jurkat cells. The experimental data were fitted using a 1 : 2 binding model,[44] indicating uneven clustering of the targets on the Jurkat and K562 cell surfaces, locally favoring multivalent interactions. The kinetic parameters like the association rate constant (k_{on}), the dissociation rate constant (k_{off}) and the dissociation equilibrium constant ($K_D = k_{off}/k_{on}$) of the interactions were calculated and the results of the interactions of WGA and SBA with Jurkat and K562 cells are shown in Table 1. The results show that the kinetic parameters are significantly different due to the difference between the k_{on} of WGA interacting with Jurkat and K562 cell surface glycans, which was much larger than that of SBA, whereas the k_{off} difference was smaller. The K_D of SBA interacting with both cells is significantly larger than that of WGA, showing the complexity and variability of cancer cell surface glycosylation.

In summary, we fabricated a dynamic reversible phenylboronic acid sensor for the real-time determination of protein–carbohydrate interactions on living cancer cell surface glycans. The living Jurkat and K562 cells were successfully captured onto the PBA-chip surface using the phenylboronic ester biomaterial interfaces that were generated by phenylboronic and *cis*-diol-containing structures on the cell surfaces. The QCM cell biosensor was used to study cell

Table 1 Dynamics and affinity of WGA and SBA interactions with Jurkat and K562 cells

	Jurkat			K562		
Lectin	k_{on} (M^{-1} s^{-1})	k_{off} (s^{-1})	K_D (nM)	k_{on} (M^{-1} s^{-1})	k_{off} (s^{-1})	K_D (nM)
WGA	1.04×10^6	2.88×10^{-3}	2.77	1.53×10^6	1.21×10^{-3}	0.79
SBA	4.38×10^4	5.27×10^{-4}	11.9	7.42×10^4	3.76×10^{-4}	5.07

surface glycosylation with several lectins, which exhibited good reproducibility. In addition, the QCM cell biosensor could be regenerated by fructose competition and PBS (pH 3.0) treatment to release the cells, which shows good regeneration for capturing different cell lines. This study provides a new method for studying living suspension cell surface glycosylation, which is of great significance for molecular recognition, cancer diagnosis and drug development.

This work was supported by the National Natural Science Foundation of China (22171230 and 21877088), the Natural Science Foundation of Hebei Province (B2019204243) and the Specialized Research Fund for the Doctoral Program of Hebei Agricultural University (ZD201712). The authors thank the State Key Laboratory of Crop Stress Biology for Arid Areas (Xiuhuan Li) and the Life Science Research Core Services (Kerang Huang), Northwest A&F University for helping with characterizations including NMR, SEM.

Conflicts of interest

There are no conflicts to declare.

Notes and references

1 G. E. Ritchie, B. E. Moffatt, R. B. Sim, B. P. Morgan, R. A. Dwek and P. M. Rudd, *Chem. Rev.*, 2002, **2**, 305–320.
2 L. Oliveira-Ferrer, K. Legler and K. Milde-Langosch, *Semin. Cancer Biol.*, 2017, **44**, 141–152.
3 I. G. Ferreira, M. Pucci, G. Venturi, N. Malagolini, M. Chiricolo and F. D. Olio, *Int. J. Mol. Sci.*, 2018, **19**, 580.
4 Y. Wu, D. C. Xiong, S. C. Chen, Y. S. Wang and X. S. Ye, *Nat. Commun.*, 2017, **8**, 14851.
5 S. S. Pinho and C. A. Reis, *Nat. Rev. Cancer*, 2015, **15**, 540–555.
6 T. Kunzke, B. Balluff, A. Feuchtinger, A. Buck and A. Walch, *Oncotarget*, 2017, **8**, 68012–68025.
7 C. H. Tsai, S. F. Tzeng, T. K. Chao, C. Y. Tsai and P. W. Hsiao, *Cancer Res.*, 2016, **76**, 5756–5767.
8 C. Gao, Q. X. Huang, C. H. Liu, C. H. T. Kwong, L. D. Yue, J. B. Wan, S. M. Y. Lee and R. B. Wang., *Nat. Commun.*, 2020, **11**, 2622.
9 L. Su, Y. Feng, K. Wei, X. Xu, R. Liu and G. Chen, *Chem. Rev.*, 2021, **18**, 10950–11029.
10 X. Liu, W. Shao, Y. J. Zheng, C. H. Yao, L. M. Peng, D. M. Zhang, X. Y. Hu and L. Y. Wang, *Chem. Commun.*, 2017, **61**, 8596–8599.
11 Z. Guo, J. X. He, S. H. Mahadevegowda, S. H. Kho, M. B. Chan-Park and X. W. Liu, *Adv. Healthcare Mater.*, 2020, **10**, e2000265.
12 R. Polsky, J. C. Harper, D. R. Wheeler, D. C. Arango and S. M. Brozik, *Angew. Chem., Int. Ed.*, 2010, **14**, 2631–2634.
13 C. Xue, S. P. Jog, P. Murthy and H. Liu, *Biomacromolecules*, 2006, **9**, 2470.
14 Y. Zhang, C. Y. Yu, E. Song, S. C. Li, Y. Mechref, H. Tang and X. Liu, *J. Proteome Res.*, 2015, **12**, 5099–5108.
15 S. Park, M. Lee, S. Pyo and I. Shin, *J. Am. Chem. Soc.*, 2004, **15**, 4812–4819.
16 J. T. Cao, X. Y. Hao, Y. D. Zhu, K. Sun and J. J. Zhu, *Anal. Chem.*, 2012, **84**, 6775–6782.
17 J. M. C. C. Guzman, L. L. Tayo, C. Liu, Y. Wang and L. Fu, *Sens. Actuators, B*, 2018, **255**, 3623–3629.
18 E. A. Smith, W. D. Thomas, L. L. Kiessling and R. M. Corn, *J. Am. Chem. Soc.*, 2013, **125**, 6140–6148.
19 H. Zhang, L. Yang, B. Zhou, X. Wang, G. Liu, W. Liu and P. Wang, *Spectrochim. Acta, Part A*, 2014, **121**, 381–386.
20 M. A. Cooper, *Nat. Rev. Drug Discovery*, 2002, **1**, 515–528.
21 Z. Pei, H. An De Rson, A. Myrskog, G. Dunér, B. R. Ingemarsson and T. Aastrup, *Anal. Biochem.*, 2010, **2**, 161–168.
22 B. Chang, M. Zhang, G. Qing and T. Sun, *Small*, 2015, **11**, 1097–1112.
23 W. He, J. Bai, X. Chen, D. Suo, S. Wang, Q. Guo, W. Yin, D. Geng, M. Wang, G. Pan, X. Zhao and B. Li, *Proc. Natl. Acad. Sci. U. S. A.*, 2022, **119**, e2117221119.
24 Y. Ma, X. Tian, L. Liu, J. Pan and G. Pan, *Acc. Chem. Res.*, 2019, **52**, 1611–1622.
25 X. L. Sun, Y. N. Jian, H. Wang, S. S. Ge, M. Yan and J. H. Yu, *ACS Appl. Mater. Interfaces*, 2019, **11**, 16198–16206.
26 P. H. Lin, S. C. Huang, K. P. Chen, B. R. Li and Y. K. Li, *Sensors*, 2018, **19**, 28.
27 P. J. Jandas, K. Prabakaran, J. Luo and M. G. Derry Holaday, *Sens. Actuators, A*, 2021, **331**, 113020.
28 Y. F. Hu, P. Zuo and B. C. Ye, *Biosens. Bioelectron.*, 2013, **45**, 79–83.
29 X. M. Li, Y. X. Pei, R. N. Zhang, Q. Shuai, F. Wang, T. Aastrup and Z. Pei, *Chem. Commun.*, 2013, **49**, 9908–9910.
30 X. M. Li, Q. Q. Song, Y. X. Pei, H. Dong, T. Aastrup and Z. C. Pei, *Sens. Actuators, B*, 2021, **326**, 128823.
31 H. Kitano, Y. Anraku and H. Shinohara, *Biomacromolecules*, 2006, **4**, 1065–1071.
32 T. Chen, P. D. Chang, T. Liu, R. Desikan, R. Datar, T. Thundat, R. Berger and S. Zauscher, *J. Mater. Chem.*, 2010, **20**, 3391–3395.
33 H. J. Liu, Y. Y. Li, K. Sun, J. B. Fan, P. C. Zhang, J. X. Meng, S. T. Wang and L. Jiang, *J. Am. Chem. Soc.*, 2013, **135**, 7603–7609.
34 G. Q. Pan, B. B. Guo, Y. Ma, W. G. Cui, F. He, B. Li, H. L. Yang and K. J. Shea, *J. Am. Chem. Soc.*, 2014, **136**, 6203–6206.
35 C. C. Lü, H. Y. Li, H. Y. Wang and Z. Liu, *Anal. Chem.*, 2013, **85**, 2361–2369.
36 A. Lennox and G. C. Lloyd-Jones, *Chem. Soc. Rev.*, 2013, **43**, 412–443.
37 G. F. Whyte, R. Vilar and R. Woscholski, *J. Chem. Biol.*, 2013, **6**, 161–174.
38 J. Yan, G. Springsteen, S. Deeter and B. Wang, *Tetrahedron*, 2004, **60**, 11205–11209.
39 L. Li, Y. Lu, Z. Bie, H. Y. Chen and Z. Liu, *Angew. Chem., Int. Ed.*, 2013, **52**, 7451–7454.
40 Y. Wang, S. Chalagalla, T. Li, X. L. Sun and X. Zeng, *Biosens. Bioelectron.*, 2010, **26**, 996–1001.
41 E. V. Chandrasekaran, J. Xue, J. Xia, S. D. Khaja, C. F. Piskorz, R. D. Locke, S. Neelamegham and K. L. Matta, *Glycoconjugate J.*, 2016, **33**, 819–836.
42 Y. Wang, X. Ao, H. Vuong, M. Konanur, F. R. Miller, S. Goodison and D. M. Lubman, *J. Proteome Res.*, 2008, **7**, 4313–4325.
43 J. Hirabayashi, H. Tateno, T. Shikanai, K. F. Aoki-Kinoshita and H. Narimatsu, *Molecules*, 2015, **20**, 951–973.
44 X. M. Li, S. Y. Song, Y. X. Pei, H. Dong, T. Aastrup and Z. C. Pei, *Sens. Actuators, B*, 2016, **224**, 814–822.

